Grant agreement no. 667510

GLINT

Research and Innovation Action
H2020-PHC-2015-two-stage

D5.4 Comparison of GlucoCEST contrast with 18F-FDG uptake

Work Package:	5
Due date of deliverable:	30/06/2018
Actual submission date:	August 19, 2018
Lead beneficiary:	UNITO
Contributors:	Anemone Annasofia, Paola Bardini, Martina Capozza, Giada Marini, Longo Dario, Aime Silvio (UNITO)
Reviewers:	Xavier Golay (UCL)

Project co-funded by the European Commission within the H2020 Programme (2014-2020)		
Dissemination Level		
PU	Public	YES
CO	Confidential, only for members of the consortium (including the Commission Services)	
CI	Classified, as referred to in Commission Decision 2001/844/EC	

*"This project has received funding from the European Union's Horizon 2020 research and innovation programme under the Grant Agreement No **667510**"*

Disclaimer

The content of this deliverable does not reflect the official opinion of the European Union. Responsibility for the information and views expressed herein lies entirely with the author(s).

*"This project has received funding from the European Union's Horizon 2020 research and innovation programme under the Grant Agreement No **667510**"*

Contents

*"This project has received funding from the European Union's Horizon 2020 research and innovation programme under the Grant Agreement No **667510**"*

1 Introduction

Positron Emission Tomography (PET) is a nuclear medicine imaging technique that is widely used in clinical practice; PET scans are utilized to estimate the metabolism in organs or tissues, so that data about their physiology and anatomy are evaluated, as well as their biochemical properties.

PET imaging is a robust modality in the imaging of primary and metastatic tumors. It has several advantages over traditional imaging techniques, including the ability to detect physiologic changes within a tumor that precede anatomic changes, and to distinguish between benign (non-cancerous) and malignant (cancerous) tumors studying the biochemical functionality. Despite the several advantages, most of the radioactive compounds used in PET imaging have a short half-life, and they are not be suitable for all patients (e.g. patients who are pregnant, suspect that they are pregnant, or are breast feeding), and PET technique is quite expensive and expose patients to ionizing radiations.

GLINT project aims to explore non-labelled glucose as a new MRI-based tracer for assessing tumor metabolism. This technology would produce an increase in safety and accessibility in comparison to PET imaging technique, as well as significant cost reductions, yet retaining and potentially increasing its specificity for the characterization of malignancy and assessment of response to therapy.

The aim of this task is to compare GlucoCEST contrast and ^{18}F-FDG-PET uptake in different tumor models to evaluate the correlation between the two measurements. These parameters will be evaluated in the same tumor after MRI and PET acquisitions, to fully explore the potentiality of this new approach.

*"This project has received funding from the European Union's Horizon 2020 research and innovation programme under the Grant Agreement No **667510**"*

2 Methodology and Approach for

2.1 Glucose preparation

Glucose solution for intravenous administration was prepared dissolving D-glucose (Sigma-Aldrich) in saline solution to obtain a 3 M solution (0.54 g/mL). The solution was then filtered with a 200 nm membrane filters in order to preserve the suspensions from bacterial contamination.

2.2 Tumour models

2.2.1 Cell culture

B16-F10 (mouse melanoma cells), 4T1 (mouse mammary carcinoma) and PC3 (human prostate cancer) cells were obtained from American Type Culture Collection (ATCC). B16-F10 cells were cultured in EMEM supplemented with 10% FBS, 100 µg/ml penicillin and 100 µ/ml streptomycin; 4T1 cells were grown in RPMI 1640 medium supplemented with 10% FBS, 100U/mL (Pen/Strep) and 2 mM L-Glutamine; PC3 cells were cultured in Ham's F-12 supplemented with 10% FBS, 100 µg/ml penicillin and 100 µ/ml streptomycin. The cells were grown at 37°C in a humidified atmosphere containing 5% CO_2.

2.2.2 Subcutaneous implantation

Male C57BL/6 mice (Charles River Laboratories Italia S.r.l., Calco Italia), female BALB/c mice (Envigo RMS, S.r.l., Udine Italia) and male Athymic Nude-Foxn1nu mice (Envigo RMS, S.r.l., Udine Italia) were maintained under specific pathogen free conditions in the animal facility of the Center for Preclinical Imaging, University of Turin, and treated in accordance with the University Ethical Committee and European guidelines under directive 2010/63. Male C57BL/6 mice were inoculated with 5.0 x 10^5 B16-F10 melanoma cells in both flanks 10 days before imaging acquisition (n=15); female BALB/c mice were inoculated with 4.0 x 10^4 4T1 cells in both flanks 15 days before imaging acquisitions (n=14); male Athymic Nude-Foxn1nu mice were inoculated with 5.0 x 10^6 cells in both flanks 30 days before imaging acquisitions (n=13).

2.3 CEST MRI protocol

Before imaging, mice were anesthetized by isoflurane, placed on the MRI bed and an air pillow placed below the animal (SA Instruments, Stony Brook, NY; USA) monitored breath rate. The tail vein was cannulated with a catheter to administer glucose through a 27-gauge needle.

*"This project has received funding from the European Union's Horizon 2020 research and innovation programme under the Grant Agreement No **667510**"*

MR images were acquired with a Bruker 7T BioSpin MRI GmbH scanner (Bruker Biospin, Ettlingen, Germany) equipped with a 30mm 1H quadrature coil.
After the scout image acquisition, T_{2w} anatomical images were acquired with a RARE sequence and the same geometry was used for the following CEST experiments.
The GlucoCEST images were obtained by irradiating the animal with a single continuous wave presaturation block pulse of 2μT applied for 5 sec. The saturation frequency offset was varied between 10 and -10 ppm with a frequency resolution of 0.2 ppm. MR images were acquired using a Spin Echo RARE sequence (TR/TE/NEX/Rare Factor 6.0 sec/4.7 msec/2/64); centric encoding, field of view = 3 cm x 3 cm; slice thickness = 2 mm; matrix = 64 x 64.
Each mouse was administered with a bolus injection of ca. 0.12 mL glucose solution at dose 5g/kg (n=8 for each tumour model).

2.4 CEST analysis

All the CEST images were elaborated in MATLAB (The Mathworks, Inc., Natick, MA, USA) using custom scripts. Anatomical and Z-spectrum images were first segmented by using an intensity-threshold filter (1). The Z-spectra were interpolated, on a voxel-by-voxel basis, by smoothing splines (2) to identify the correct position of the bulk water, thus removing artefacts arising from B_0 inhomogeneity. On this basis, the interpolated Z-spectrum was shifted so that the bulk water resonance corresponds to the zero frequency and corrected intravoxel saturation transfer (ST) effects were calculated. Then, a second filter was applied to remove CEST effect arising from noisy data, calculating the coefficient of determination R^2 for the interpolating curve to take into account the signal-to-noise ratio of single voxels (noisy Z-spectra present low R^2 values). Only voxels with high R^2 (>0.99) were considered in the ST% calculation.

The ST effect for glucose was estimated from the expression:

$$ST = \frac{S(-1.2ppm) - S(1.2ppm)}{S_0} \qquad [1]$$

where S_0 was the signal at -10ppm.
Results are reported as:

$$\Delta ST\ \% = [(\text{ST post injection} - \text{ST pre injection}) * 100]$$

The fraction pixel ST reports on the percentage of pixels showing a ΔST% above the threshold (2 %) in the manually-defined tumour region of interest (ROI).

*"This project has received funding from the European Union's Horizon 2020 research and innovation programme under the Grant Agreement No **667510**"*

2.5 PET protocol and Analysis

Animals were imaged two days after the MRI imaging acquisition and were kept fasting overnight before the intravenous ^{18}F-FDG injection (8.66±0.64 MBq/mouse). The injected dose was calculated by the difference of the radioactivity in the syringe before and after the administration, as measured by a dose calibrator (IsoMED 2010, MED Nuklear-Medizintechnik Dresden GmbH). Animals were anesthetized with isoflurane (3-4% for induction, 1%-1.5% for maintenance, in oxygen) and then placed in a dedicated small-animal multimodality scanner (Triumph II, TriFoil Imaging, Chatsworth, CA), equipped with inhalation anesthesia and heating pad. Instrument calibration was performed with phantoms containing small known amounts of radioactivity.

A whole-body CT scan was performed immediately before the PET acquisition in order to provide anatomical information (512 projections, 1 frame per projection, 75 kV peak tube voltage, 150 mA tube current, 230 ms exposure time). PET static acquisition was performed for 30 minutes starting 45 minutes after probe administration. PET and CT images were reconstructed using the LabPET software (TriFoil Imaging), all images were corrected for decay and tissue attenuation, and the CT data were used to provide attenuation correction. The PET data were reconstructed in a single frame using a 3D algorithm (Ordered Subset Expectation Maximization, OSEM-3D) with 8 subsets and 10 iterations. Reconstructed and co-registered PET/CT images were quantitatively evaluated using the AMIDE software package, by drawing volumes of interest (VOIs, thickness 1 mm) over tumors on axial images. PET data are expressed as percentage of injected dose per cubic centimeter (%ID/cc), standardized uptake values (SUV) and maximum standardized uptake values (SUVmax). SUV and SUVmax were calculated using the formula: SUV = mean activity in the volume of interest/(injected dose/body weight) and SUVmax = maximum activity in the volume of interest/(injected dose/body).

*"This project has received funding from the European Union's Horizon 2020 research and innovation programme under the Grant Agreement No **667510**"*

3 Report Activities carried-out and results

To investigate the correlation between GlucoCEST contrast and ^{18}F-FDG uptake, CEST images of three different tumour models (B16-F10, 4T1 and PC3) were acquired on a 7T scanner, before and after glucose injection; two days after MRI acquisition mice were kept overnight fasted and injected with ^{18}F-FDG in order to perform PET imaging.

In MRI experiments each mouse was intravenously administered with 5g/Kg of glucose solution.

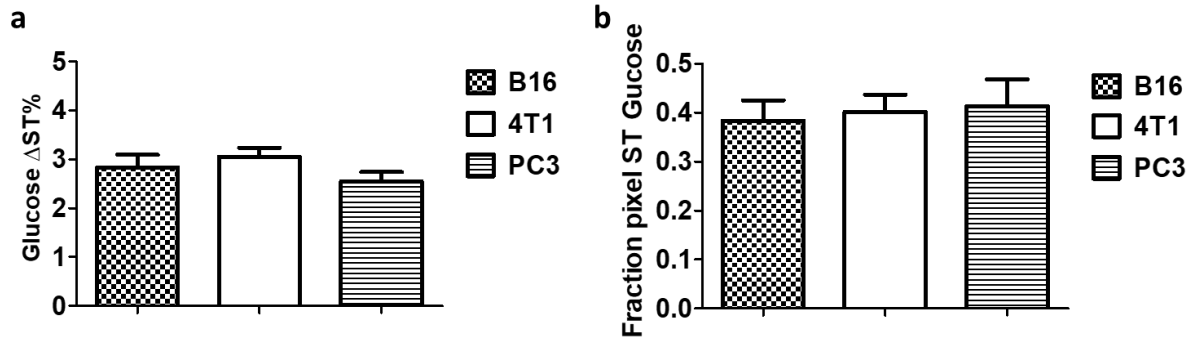

Figure 1: **a**, Bar graph showing mean ± SD GlucoCEST contrast obtained injecting glucose solution at 5g/Kg dose via intravenous bolus for each tumour model. Data are reported as the variation (ΔST%) between the ST effect percentage post minus pre intravenous injection. **b**, Bar graph showing mean ± SD Fraction pixel for each tumour model that detected glucose contrast above 2% threshold.

As shown from the mean value graph in **Figure 1** and from representative contrast map in **Figure 2** (left panel), the three tumour models displayed a similar GlucoCEST contrast (glucose ΔST% = 2.83, 3.04 and 2.54 for B16-F10, 4T1 and PC3, respectively). A lower, but not statistical significant GlucoCEST contrast was observed for the PC3 tumor model in comparison to the other tumor models. The fraction pixel value for all the tumour models investigated is around 0.4, showing that 40% of the pixels inside the selected ROI revealed a detectable signal (ΔST% > 2%) from glucose.

Two days after the MRI acquisitions the PET/CT imaging was performed. Scans were acquired 45 minutes after ^{18}F-FDG administration. PET analysis was carried out on whole tumours, and representative images of the tumours, corresponding to the MR imaging tumours slices, are reported in the right panel of **Figure 2**.

*"This project has received funding from the European Union's Horizon 2020 research and innovation programme under the Grant Agreement No **667510**"*

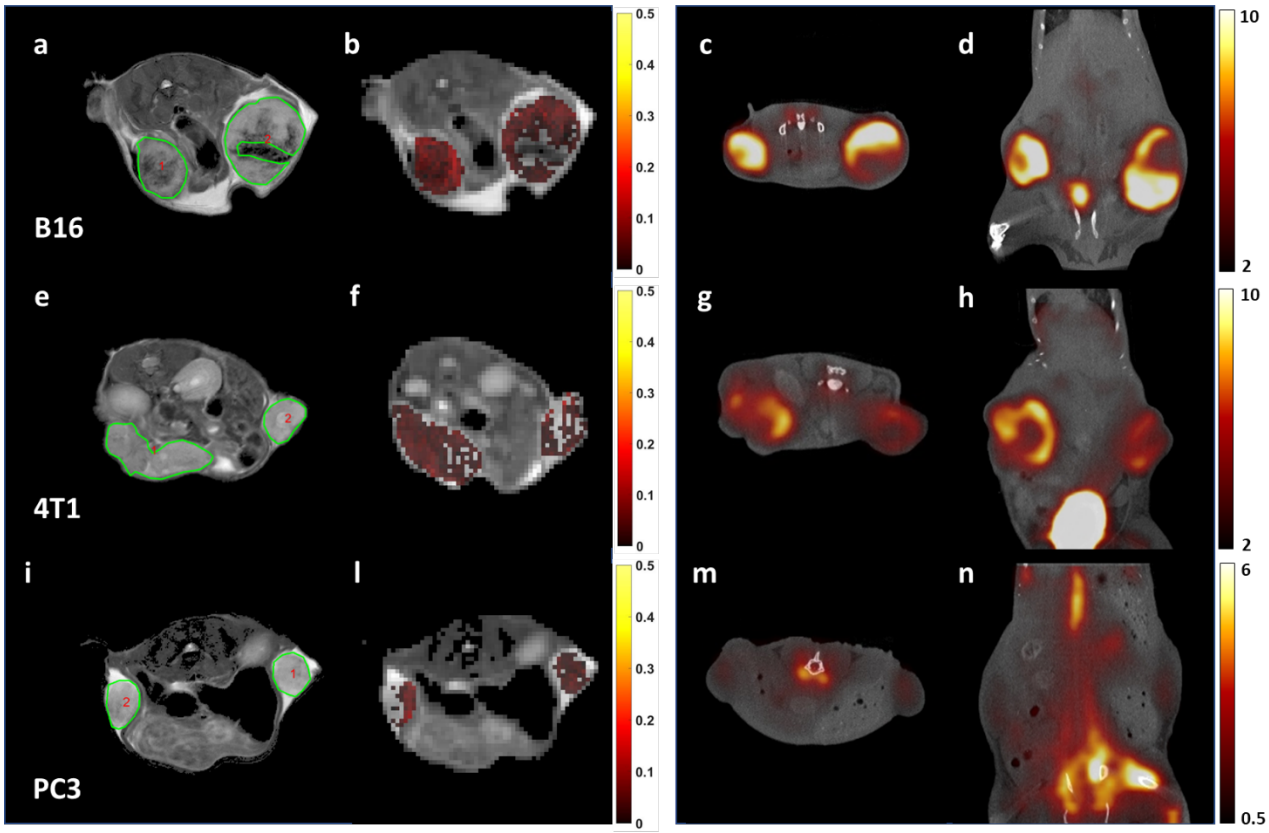

Figure 2: **a**, **e**, and **i**, Anatomical T_2 weighted images of representative B16-F10, 4T1 and PC3 tumour bearing mice. **b**, **f**, and **l**, Representative GlucoCEST map overimposed on the anatomical image of each tumour model obtained after i.v. injection of D-glucose, 5 g/kg (Data are reported as the difference, ΔST %, between the ST effect before and after the intravenous injection). **c**, **g**, and **m**, Fused PET/CT axial view images and **d**, **h**, and **n** Fused PET/CT coronal view images of representative B16-F10, 4T1 and PC3 tumour bearing mice injected with ^{18}F-FDG. Data are expressed as % ID/cc.

We observed that the uptake of ^{18}F-FDG was significantly higher in B16-F10 (SUV: 0.91, SUV max: 2.08 and %ID/cc: 3.67) and in 4T1 (SUV: 0.62, SUV max: 1.09 and %ID/cc: 3.23) tumours than in PC3 tumours (SUV: 0.32, SUV max: 0.46, %ID/cc: 1.15) (**Figure 3**).

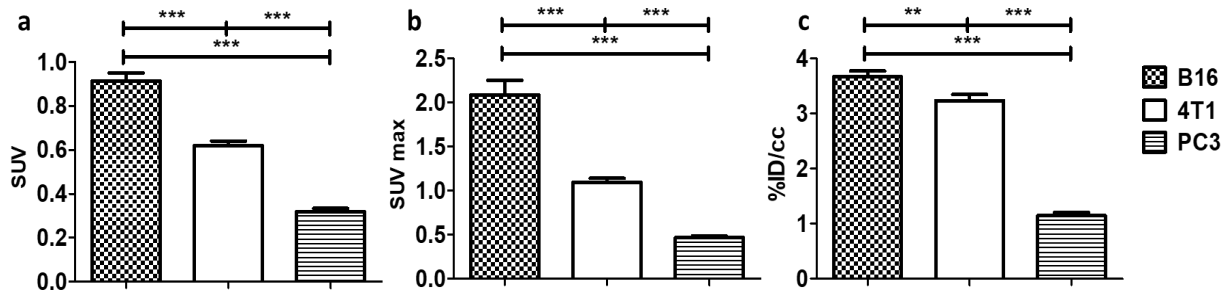

*"This project has received funding from the European Union's Horizon 2020 research and innovation programme under the Grant Agreement No **667510**"*

Figure 3: ^{18}F-FDG PET/CT uptake for each tumour model. Bar graphs showing mean ± SD standardized uptake values (SUV, a), maximum standardized uptake values (SUVmax, b) and injected dose per cubic centimeter (%ID/cc, c) values. **, P <0,01. ***, P<0,001.

In addition to the MRI and PET/CT average analysis, a correlation analysis was performed on both averaged MRI-based and PET-based estimates. As reported in **Figure 4**, there was a significant and inverse correlation between GlucoCEST contrast and FDG uptake only in the B16-F10 tumor model, whereas no significant correlations were observed with the other tumor models.

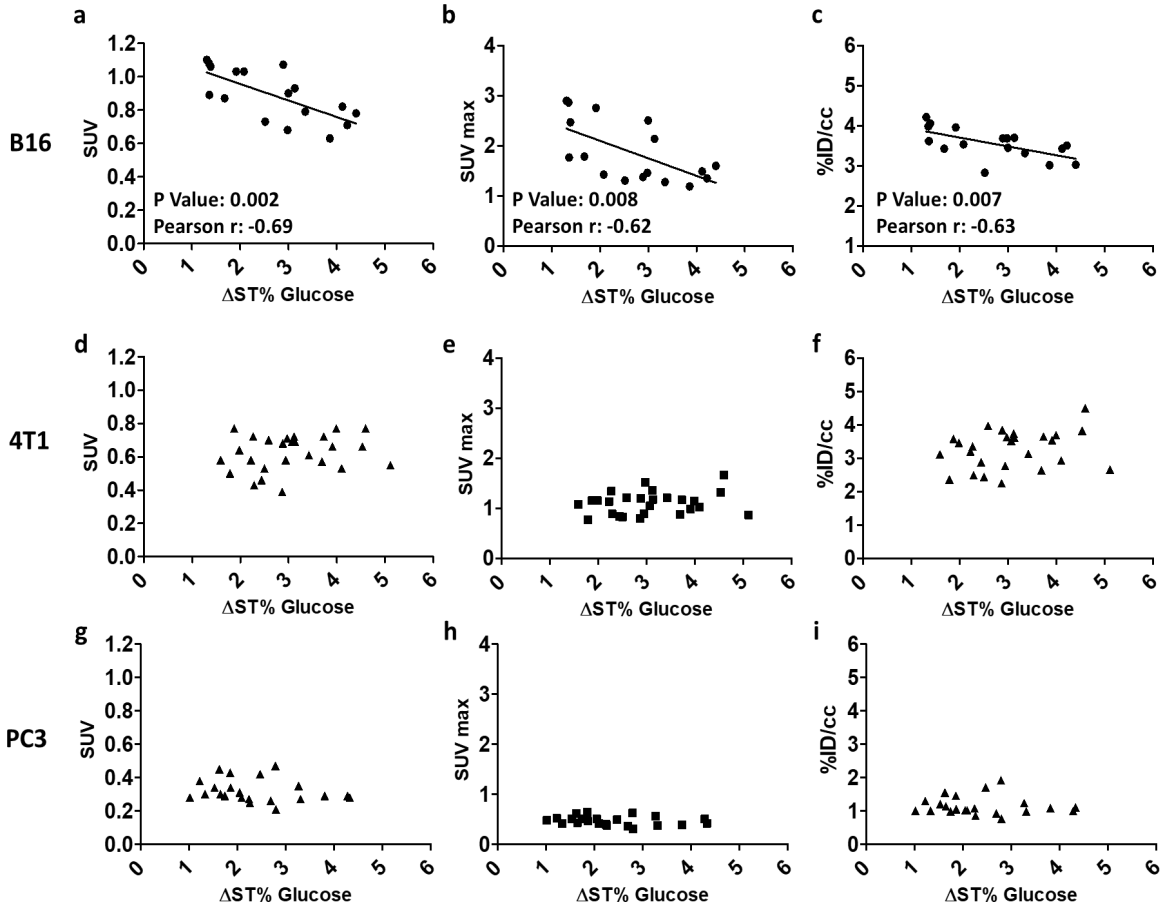

Figure 4: Correlation between GlucoCEST ΔST% contrast and SUV values (a, d and g), SUVmax values (b, e and h), %ID/cc values (c, f and i) among the three tumour murine models. $p < 0.05$ was regarded as statistically significant.

*"This project has received funding from the European Union's Horizon 2020 research and innovation programme under the Grant Agreement No **667510**"*

4 Conclusions

The aim of this task was to compare the GlucoCEST contrast by MRI with the uptake of the ^{18}F-FDG by PET imaging. In order to fully explore the capability of the GlucoCEST method, three different and representative tumour models have been investigated: murine melanoma (B16-F10), murine breast (4T1), and human prostatic cancer (PC3) in male C57BL/6 mice, female BALB/c mice, and male Athymic Nude-Foxn1nu mice, respectively. GlucoCEST and ^{18}F-FDG-PET acquisitions were performed on the same mice, two days apart from each other and the averaged values for both the MRI and PET estimates were compared.

The three tumor models showed a marked different FDG uptake, that was lower for the prostate one. A similar trend was observed for the GlucoCEST technique, with lower GlucoCEST contrast for the PC3, despite not statistically significant. However, when correlating in the same tumors the glucoCEST contrast vs. the PET-based estimates, no clear correlation was observed for the three tumor models. We have to acknowledge several limitations in our study that may explain this lack of correlation between the MRI-based and PET-based estimates. First, the GlucoCEST contrast has been measured only in the central slice of the tumor, whereas the PET estimates have been calculated as an average over the whole tumor. As a consequence, the averaged values of the GlucoCEST contrast could not be truly representative for the whole tumour. Second, the two measurements have been acquired in different days, so despite the tumor growth rate was low, some physiological changes may happen within the tumors. Third, the glucose infusion has been done with mice that have not been fasted the night before, whereas for the FDG infusion the mice have been fasted. Therefore, some differences in the glucose uptake may be expected, despite a marked GlucoCEST enhancement was observed with the MRI-CEST approach (mean ST% difference between post and pre injection values was of ca. 3%) reflecting enough glucose accumulation within the tumor.

To conclude, further investigations are needed to better understand the different factors, including physiological differences related to the tumour models as well as to the information provided by the GlucoCEST technique in comparison to the standard FDG-PET approach.

*"This project has received funding from the European Union's Horizon 2020 research and innovation programme under the Grant Agreement No **667510**"*

5 Bibliography / References

1. Chu V, Hamarneh G. MATLAB–ITK interface for medical image filtering, segmentation, and registration. Proc SPIE Med Imaging: Image Process 2006;6144:1–8.

2. Stancanello J, Terreno E, Castelli DD, Cabella C, Uggeri F, Aime S. Development and validation of a smoothing-splines-based correction method for improving the analysis of CEST-MR images. Contrast Media Mol Imaging 2008;3:136–149.

*"This project has received funding from the European Union's Horizon 2020 research and innovation programme under the Grant Agreement No **667510**"*